

Measurements of Randomly Placed Wireless Transmitters Used as an Array for Receivers Located Within the Array Volume With Application to Emergency Responders

William F. Young, *Member, IEEE*, Edward F. Kuester, *Fellow, IEEE*, and Christopher L. Holloway, *Senior Member, IEEE*

Abstract—Emergency responders often experience poor quality wireless communications due to the complex radio-frequency propagation environment encountered at a typical emergency response location, such as an apartment complex, office building, or other large building structure. Our previous theoretical analysis in conjunction with simulation studies suggests that optimizing arrays of randomly located wireless transmitters can provide a significant increase in the received signal level for a receiver located in the array volume. Here we present experimental results from the application of our initial algorithm in representative complex propagation environments. Several different scenarios are included in the experiments to demonstrate the effectiveness of the optimization approach in an environment that contains a variety of scattering objects. For the various scenarios, we observed at least a 7 dB median gain over a single transmitter when the array consists of four transmitters.

Index Terms—Ad hoc array, arbitrary array optimization, emergency responder communications, random array.

I. INTRODUCTION

WIRELESS communication represents a key supporting technology for the success of an emergency responder [1]. Unfortunately, a typical emergency response scenario involves communication into building structures, which can severely interfere with or completely block radio-frequency (RF) communications. As we proposed in [2], one potential method of improving the RF channel within a building utilizes the intelligent control of the electromagnetic radiation from wireless devices quickly placed at random locations in the building during entry by the emergency responder. These devices would perform as antenna array elements to improve communication capability for emergency responders both within the structure and with external personnel. In this paper,

Manuscript received August 10, 2007; revised August 11, 2008. Current version published March 04, 2009. This work was supported in part by Sandia National Laboratories, Albuquerque, NM, and in part by the National Institute of Standards and Technology, Gaithersburg, MD.

W. F. Young is with the Sandia National Laboratories, Albuquerque, NM 87185-0986 USA (e-mail: wfyong@sandia.gov).

E. F. Kuester is with the Department of Electrical and Computer Engineering, University of Colorado Boulder, CO 80309-0425 USA.

C. L. Holloway is with the National Institute of Standards and Technology, Boulder, CO 80305-3328 USA.

Color versions of one or more of the figures in this paper are available online at <http://ieeexplore.ieee.org>.

Digital Object Identifier 10.1109/TAP.2008.2009651

we present experiment results that implement the proposed algorithm in our earlier work [2], with the inclusion of additional representative boundary configurations beyond those used in the initial simulation results.

Array directivity or gain optimization techniques based on a generalized matrix eigenvalue problem are well covered in past literature, [3]–[7], with [8]–[10] focused on constrained optimization. All these works assume a receiver in the far-field rather than within the volume of the array, as was the case of [2]. A method for adapting radiated power for receivers located in the near-field is discussed in [13], but more relevant to our work, [14] discusses optimizing arrays in arbitrary environments. However, neither [13] nor [14] contains experimental results with a receiving antenna located within the array volume.

The remainder of this paper proceeds as follows: Section II outlines the implementation algorithm, Section III describes the experiment, Section IV shows the experimental results, and Section V contains our conclusions.

II. WIRELESS ARRAY IMPLEMENTATION

The simulation results in our earlier work [2] and [15] point out some key impacts to field-implementation. First, diminishing returns in total received power occur after the array contains a small number of transmitters, approximately four transmitters for the optimized case and six to eight transmitters for the co-phased case. (Co-phasing means adjusting the transmitted signal phase such that all the received signals have the same phase, e.g., [16], [17].) Second, for this same small number of transmitters, the modified directivity results [[2], (11)] are not significantly different for the optimized and co-phased results. Thus, we propose the following algorithm to obtain the co-phased results, with the recognition that the algorithm also provides a reasonable approximation of the optimized modified directivity.

- 1) Turn on each transmitter individually, and determine the transmitter providing the maximum contribution at the receiver.
- 2) Select the strongest contributing transmitter, and turn it on with all the others off.
- 3) Select the next strongest transmitter determined in Step 1, and turn it on.

TABLE I
PERFORMANCE PARAMETERS OF DIGITAL PHASE SHIFTERS

Part Number	Center frequency	Maximum switching time	Maximum insertion loss
DP-2-4-290-10-73 [19]	290 MHz	100 ns	4 dB
CDP0926 [20]	1.3 GHz	3.5 μ s	3 dB
ACPS-A629 [21]	3 GHz	200 ns	3.5 dB

- Step the phase of this transmitter through 360° , and determine the phase when the peak power occurs at the receiver.
 - Set the phase of this transmitter to that corresponding to the maximum power at the receiver.
- 4) Repeat Step 3 for the remaining transmitters, until the desired number of contributing transmitters is reached.

This process will ensure co-phased transmitted signals at the receiver for however many transmitters are used in the array. If total system or radiated power is not a limitation, all the co-phased transmitters could be included in the process. However, if system power efficiency is important, say for example in a low power sensor network, then the optimized approach represents a more appropriate solution because it balances the power received at a particular location with the total system input power.

The optimization process reduces the power level of transmitters providing the weakest contribution at the receiver, which suggests only using the four or so strongest contributing transmitters. A reasonable approximation of the optimized solution is to use the algorithm above for a limited number of transmitters. To obtain the complete optimized result, the relative power level of each transmitter could potentially be adjusted by an additional iterative algorithm.

As we will discuss in Section IV, near optimal results do not require precise phase control. A 4-bit phase shifter, which covers the full 360° sweep in sixteen 22.5° increments, will allow reasonable sweep and phase switching times. Table I below lists some typical digital phase shifter performance values.

Timing estimates for the key parts of the algorithm are as follows. Use the highest value of switching time, 3 μ s, select the four strongest transmitters, and then co-phase the selected four to obtain the following result.

$$\text{test transmitters} + 3 \mu\text{s} \times [4 \times 16] = \text{test time} + 192 \mu\text{s} \quad (1)$$

The setup time required depends primarily on measuring the individual transmitter levels. Feedback information would need to tell each transmitter which phase achieved a maximum value. While the emphasis of this work is not on the setup protocol design, we estimate that approximately 20 bits of information will allow identification of each transmitter and selection of the appropriate phase for that transmitter.

III. EXPERIMENT DESCRIPTION

The experimental configuration consists of randomly located $\lambda/4$ monopoles on an aluminum ground plane, where the antennas serve as transmitting array elements and a single

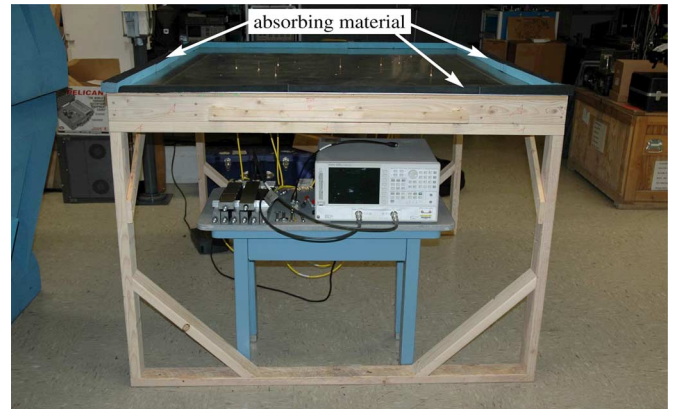


Fig. 1. Array configuration in the laboratory with an absorbing border, but no concrete block walls.

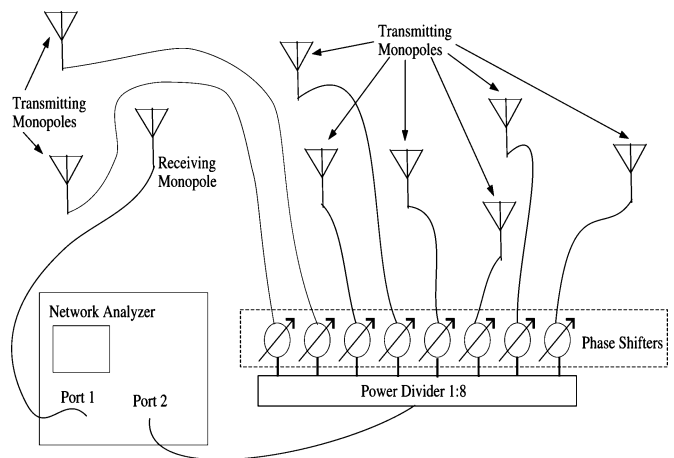


Fig. 2. Sketch of experimental configuration.

receiving antenna. This configuration approximates dipoles in free space when no obstacles are present on the ground plane. The ground plane is mounted on wooden legs, and the test equipment is placed under the ground plane, (see Fig. 1). A network analyzer provides both the transmitted power source and received power measuring device. Fig. 2 illustrates the basic experimental configuration, while pictures of the actual components are shown in shown in Fig. 3 (except for the monopole antennas). Port 2 of the network analyzer feeds a power divider, which provides equal power to the monopoles comprising the array of transmitters. Mechanical phase shifters, tunable over 360° at 2 GHz, are located between the power divider and the individual transmitting monopoles. Port 1 of the network analyzer connects to a single monopole, which represents the receiver. Additional details on the experiment are contained in Chapter 5 of [18].

In [2], we applied three measures of performance: 1) modified directivity [2], (11), 2) total power at the receiver [2], (30), and 3) power per transmitter at the receiver [2], (31). Here we utilize the second two performance measures. The measurement results from the experiments are presented as 1) total received power, 2) total normalized received power, and 3) normalized power per transmitter. The normalization allows for comparison to free space simulation results.

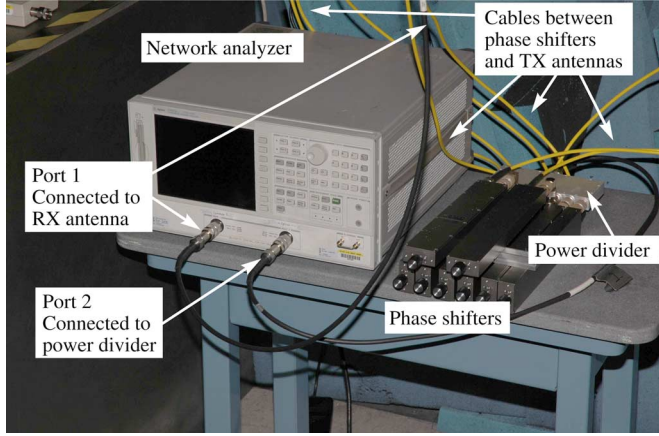


Fig. 3. Picture of experimental setup. There are eight phase shifters connected between the 1:8 power divider and the eight transmitting antennas of the array.

Total measured power P_{tot} , is obtained from the ordered cumulative sum of the received power due to the M strongest transmitters, up to the total number of available transmitters, N . Nine different experiments (referred to as scenarios or cases), are performed here and discussed below. For these experiments, $N = 8$, except for case 1 where $N = 7$

$$P_{\text{tot}} = \sum_{i=1}^M P_i^{\text{meas}}, P_1^{\text{meas}} \geq P_2^{\text{meas}} \dots \geq P_M^{\text{meas}}$$

where $i = 1, 2, \dots, M$ and $M \leq N$. (2)

Any transmitters not included in the sum, i.e., $M < i \leq N$, are disconnected from the power source. The median value is then calculated for ten different receiver locations, across a fixed number of contributing transmitting monopoles.

The total normalized measured power $P_{\text{tot}}^{\text{norm}}$, is determined by first computing the median statistics for a fixed number of transmitting monopoles across the ten different receiver locations, and then dividing by the single transmitting monopole results. Normalized measured total power is computed as

$$P_{\text{tot}}^{\text{norm}} = \frac{P_{\text{tot}}}{P_1^{\text{meas}}}. \quad (3)$$

Thus, the median curves start at 0 dB for a single transmitter. Note that $P_{\text{tot}}^{\text{norm}}$ is computed independently for each scenario. Normalized power per transmitter is calculated by dividing $P_{\text{tot}}^{\text{norm}}$ by the number of transmitting monopoles M , included in the sum

$$P_{\text{transmitter}}^{\text{norm}} = \frac{P_{\text{tot}}^{\text{norm}}}{M}. \quad (4)$$

An experimental scenario or case consists of carrying out the co-phase algorithm discussed in Section II to achieve maximum gain at the receiving antenna for each of the ten different receiver locations (except for cases eight and nine). One of the primary goals of the experiments is to study differences in array behavior due to boundaries or obstacles in the environment. The nine different cases include a variety of objects on the ground plane in order to approximate array performance in free space

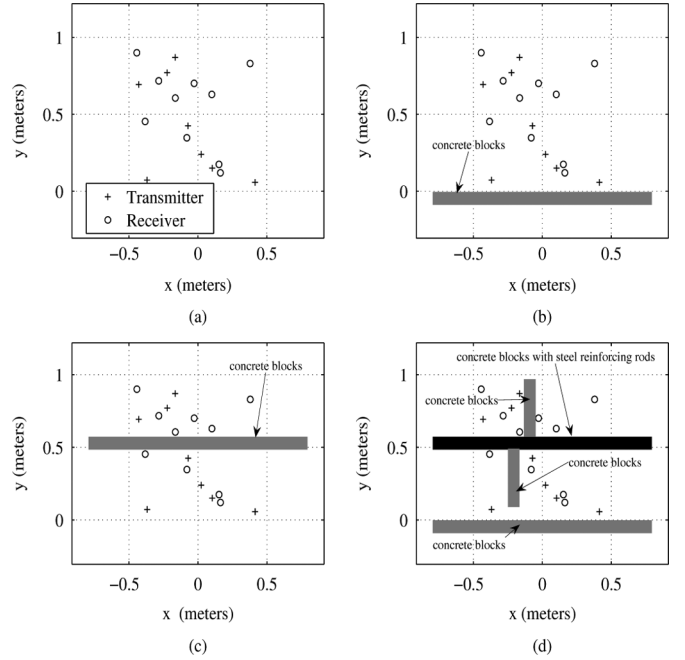


Fig. 4. Top view of experiment topology for monopoles on the ground plane.



Fig. 5. Array configuration in anechoic chamber with concrete block wall on the border of the array and an absorbing border on the ground plane.

and building environments. Transmitting array antennas reside at the same locations and the same ten receive locations are utilized for all nine cases. The order in which the transmitting antennas are added to the array, as well as the performance results, vary due to the inclusion of items such as concrete blocks and reinforcing bars. Table II provides details of the nine experimental scenarios, where the topology drawing (Fig. 4) and pictures (Figs. 1, 5, and 6) illustrate some important features of the experiment. (The absorbing border is carbon loaded foam designed for anechoic chambers, and is used here to minimize the edge effect of the ground plane.)

As indicated by the algorithm, the first step is to rank the signal strength for each individual transmitting antenna at a particular receive antenna location. To this end, the array of transmitting antennas are connected one at a time, with all other cables from the remaining seven phase shifters terminated

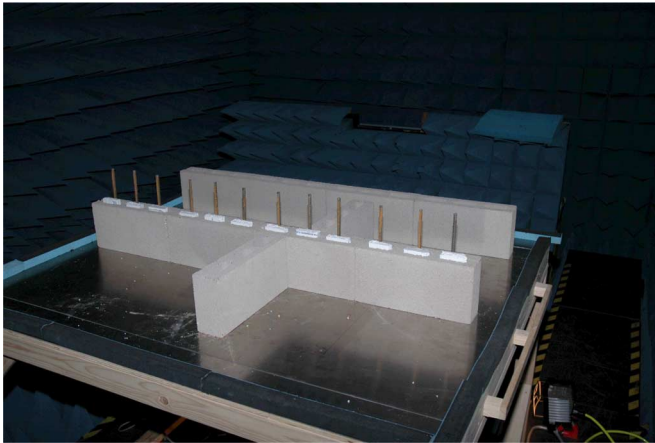


Fig. 6. Array configuration in anechoic chamber with multiple concrete block walls and an absorbing border on the ground plane. The center wall contains reinforcing rods.

TABLE II

EXPERIMENTAL SCENARIOS PERFORMED IN A LAB ROOM (LR) AND AN ANECHOIC CHAMBER (AC). ‡ INDICATES OMISSION OF CO-PHASING TO ACHIEVE MAXIMUM GAIN AT THE RECEIVER

Number	Location	Absorbing border	Topology	Picture
1	LR	no	Fig. 4(a)	none
2	LR	yes	Fig. 4(a)	Fig. 1
3	AC	no	Fig. 4(a)	none
4	AC	yes	Fig. 4(a)	none
5	AC	yes	Fig. 4(b)	Fig. 5
6	AC	yes	Fig. 4(c)	none
7	AC	yes	Fig. 4(d)	Fig. 6
8‡	LR	no	Fig. 4(a)	none
9‡	LR	no	Fig. 4(d)	none

in 50Ω loads. After establishing the order, the monopole antennas of the array are connected sequentially from strongest to weakest. When an antenna is connected to the power divider, thus becoming part of the array, the phase of the now radiating monopole is tuned via the corresponding phase shifter in order to maximize the total received power at the receiving antenna. The complete process is repeated for the ten different receive antenna locations.

For cases eight and nine, the transmitter phases are not adjusted as the transmitters are added to the array so as to emulate an uncontrolled or random operation of the array. The order in which the transmitters are added to the array in cases eight and nine is identical to cases one and seven, respectively. This provides additional insight into the benefit provided by performing the optimization process.

The network analyzer supplies a 0 dBm signal to the power divider through port 2, and the received power is computed from the resulting s_{12} value at port 1. While the amount of loss introduced by the cables, connectors, and the power divider are not accounted for in the calibration process, the s_{11} and s_{22} values are checked after each connection to verify good matches between the two ports and the receive antenna and transmitting array, respectively. Typical values for s_{11} and s_{22} indicate matches of better than -19.5 dB and -21.0 dB, respectively.

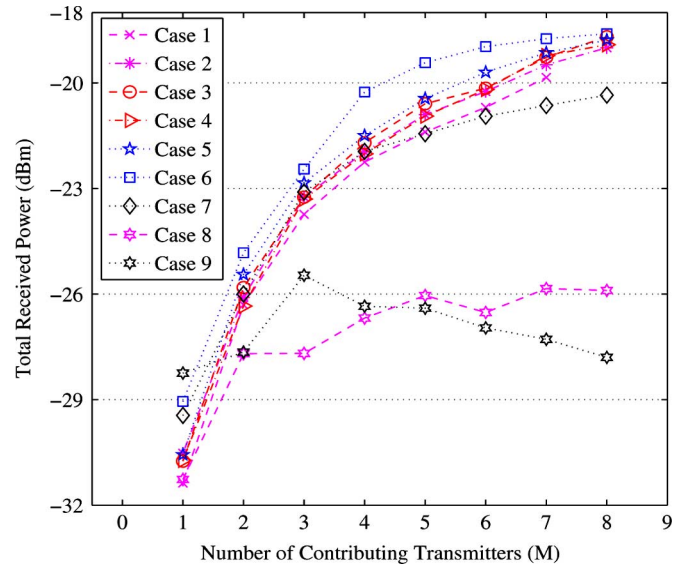


Fig. 7. Median total power results from the measured data.

The worst mismatch between the network analyzer and the array feed structure is $s_{22} = -20.0$ dB, while the worst mismatch to the receive antenna is $s_{11} = -15.8$ dB. This later case occurs due to the proximity of the receive antenna location and the concrete block wall containing steel reinforcing bars. However, even the worst case mismatches do not appear to affect the outcomes of the experiments, as demonstrated by the results that follow.

IV. EXPERIMENTAL RESULTS

The experimental results in Fig. 7 show the median values of the total power (2) for the nine scenarios or cases. Note that the total power is measured in dBm due to the 0 dBm source at port 2 of the network analyzer. Across all numbers of contributing transmitters for the first seven cases, the spread between the median gain is less than 3 dB. The first five cases exhibit a spread of approximately 1 dB, which is expected since no obstacles are placed in the volume of the array. Cases six and seven include concrete block walls within the volume of the array, which results in additional spreading of the median total power. The overall increase in total power shown in case six is likely due to the constructive interference caused by reflections from the concrete wall in conjunction with the minimal amount of attenuation caused by the concrete blocks. Case seven demonstrates a decrease in the rate of gain as the number of included transmitters is increased, which is likely due to the scattering caused by the reinforcing bars and the additional concrete blocks in the array environment. Cases eight and nine indicate that simply adding up the transmitter contributions without phase adjustment provides virtually no benefit. The behaviors of cases eight and nine are quite similar, even though case eight contains no scatterers within the array volume, while case nine utilizes the scatterer topology illustrated in Fig. 4(d).

The same set of experimental results are shown in Fig. 8, but are normalized to allow comparison to simulated results, i.e., (3). In the simulation, the transmitting and receiving antennas

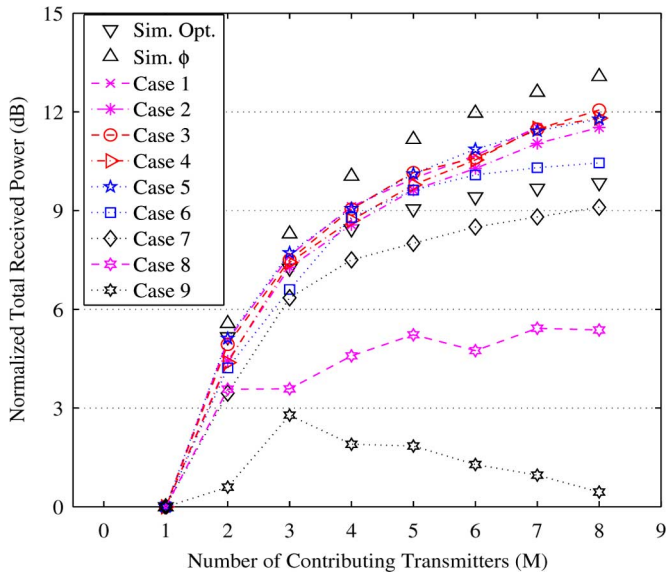


Fig. 8. Median total power results from the measured data and simulations, normalized to 0 dB for a single transmitter.

are Hertzian dipoles assumed to exist in free space. (See [2] and [18] for simulation details.)

The first observation is that cases one through six fall between the co-phased and optimized results, but cases seven, eight and nine fall below the optimized results. This behavior is expected for cases eight and nine, as no phase control was carried out. In case seven, the curve follows the optimized result, but with about 1 dB of attenuation. The second observation is that the curves for the first five cases follow the same general shape as the simulated co-phased case, which is expected since only phase control is used in the experiments. Finally, we observe that as obstacles are introduced into the volume of the array, (cases six and seven), the behavior follows that of the simulated optimized results. This is due to the attenuation caused by the obstacles, which creates an impact similar to controlling the power amplitude in the optimized approach.

A third set of experimental results shown in Fig. 9 depicts the normalized power per transmitter (4), and again the general trends are comparable between measured and simulated cases. Fig. 9(a) includes the complete set of experimental and simulated results, while Fig. 9(b) provides an expanded view of the 0–5 dB ordinate range. The first five cases indicate less than a 0.5 dB spread across all numbers of contributing transmitters, and a maximum difference of approximately 1.5 dB with the simulated co-phased results. Both the measured and simulated co-phased curves flatten by the time four transmitters are included in the array. Cases six and seven do not track the simulated optimized results quite as well in terms of spread, but the general trends are quite similar. The simulated optimized and scenarios six and seven results show a maximum at either three or four transmitters in the array, followed by a decrease as the number of transmitters increases. The rate of decrease tracks quite well between these three cases.

Fig. 10 shows the average distance between the receiver and the transmitter for the first seven cases. In this plot, the number on the abscissa refers to the order or the index, i , in which the

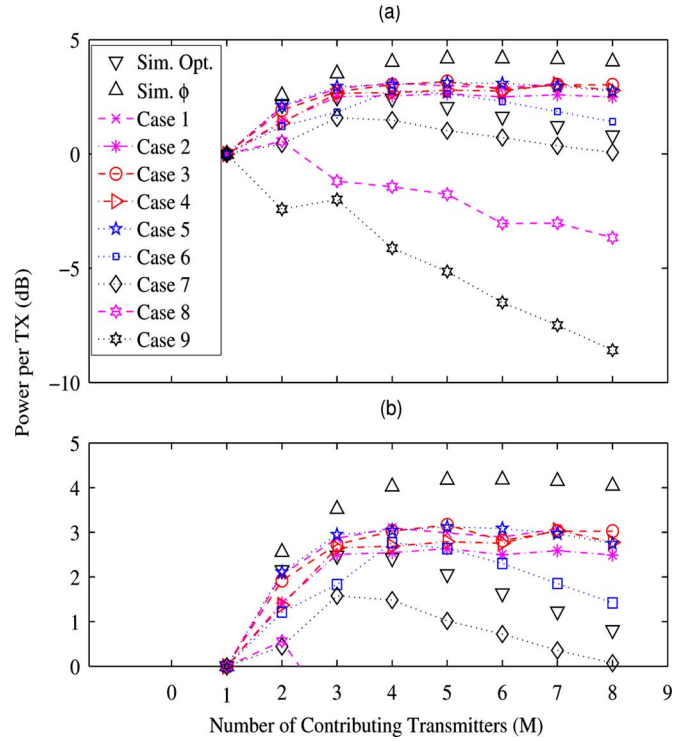


Fig. 9. Power per transmitter results from the measured data and simulations, normalized to 0 dB for a single transmitter.

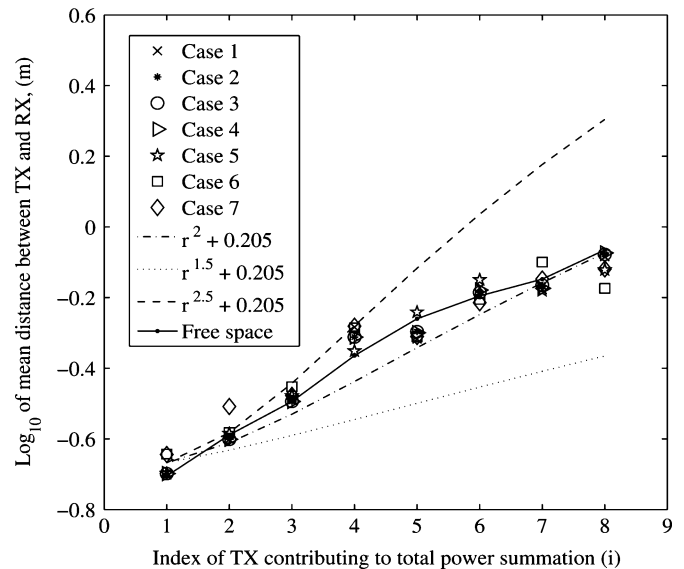


Fig. 10. Average separation between the TXs and RXs as a function of the transmitter index in the total power sum. Log_{10} distance scale.

transmitter is included in the array. The ordinate measure shows the logarithmic mean distance between the receiver location and the particular transmitter location. For example, the abscissa value of two refers to the second transmitter of the array, and averaging over the ten receiver locations for case seven yields a value of approximately 0.3 m. The free space plot in Fig. 10 shows the average distance with respect to signal strength that would be observed in ideal free space, but with the location restrictions imposed by the random locations used in the experimental setup. Fig. 10 includes $r^{1.5}$, r^2 , and $r^{2.5}$ curves as well

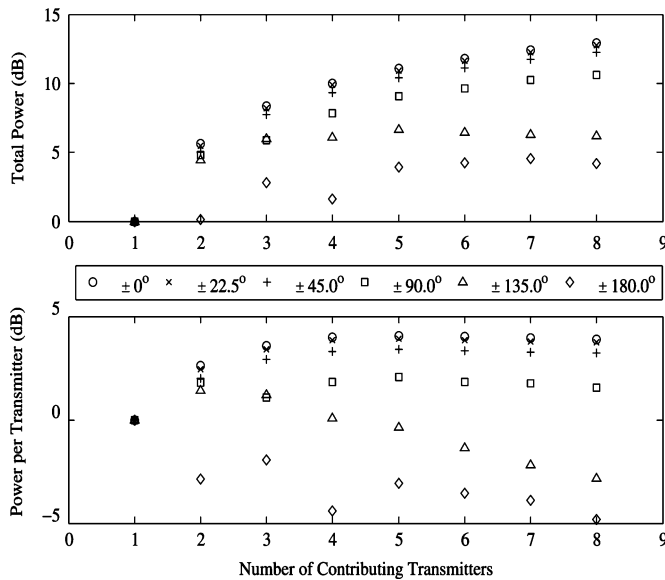


Fig. 11. Random additional phase offsets in co-phased simulations used for experimental data comparisons. Total normalized power and power per transmitter simulation results, normalized to 0 dB for a single transmitter.

to demonstrate the general r^2 behavior of the array. For the seven cases, the obstacles do not significantly affect the order in which transmitters are included in the sum, at least in the average distance sense. The obstacles do not introduce significant segmentation of the array. Segmentation occurs when the transmitters located within a local region bordered by walls provide the majority of power at the receiver, particularly when the receiver is located in the local region. If the walls created either higher signal attenuation or stronger reflections, then much greater array segmentation is likely.

Finally, we observed that the phase adjustment process was not highly sensitive to the mechanical knob rotation as evident by the ease in obtaining the power maximum as transmitting monopoles were added into the array. Fig. 11 shows results where simulated co-phased currents received additional phase offsets, e.g., $\pm 22.4^\circ$. The results indicate that for even up to $\pm 45^\circ$, most of the gain is still realized. Additional simulation studies included in [18] also suggest that a 22.5° incremental step will still achieve almost all the realizable gain. This minimal degradation in performance can be viewed as similar to Fresnel zone behavior, where a variation of $\pm 90^\circ$ corresponds to a range of $\lambda/2$, and hence no destructive interference occurs. Therefore, we suggest that for a narrow band system a 4-bit phase-shifter can provide the necessary phase control.

V. CONCLUSION

Our initial research into optimizing arbitrarily located wireless arrays suggested an algorithm for implementing such an array. The experimental results presented here were obtained by carrying out the algorithm in environments more complex than those explored in the original simulations. However, the array still performs as anticipated, and suggests that the proposed optimization can support improved communications

within complex RF environments. Observations during the experiments and further simulation results suggest that only 4-bit delineation in the phase-shifting is necessary to achieve most of the realizable gain. Further research and development activities into necessary communication protocols and hardware platforms are still required, but both the initial simulation studies and these subsequent experimental results establish the foundation for follow-on efforts towards a deployable system.

ACKNOWLEDGMENT

The authors thank G. Koepke of NIST for his guidance and suggestions in carrying out these experiments, and R. Wittmann of NIST for useful technical discussions.

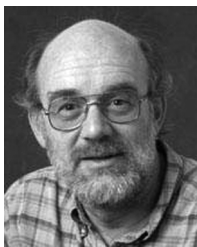
REFERENCES

- [1] L. E. Miller, "Wireless technologies and the Safecom SoR for public safety communications," National Institute of Standards and Technology, Gaithersburg, MD, 2005 [Online]. Available: <http://www.antd.nist.gov/wctg/manet/docs/WirelessAndSoR060206.pdf>
- [2] W. F. Young, E. F. Kuester, and C. L. Holloway, "Optimizing arrays of randomly placed wireless transmitters with receivers located in the array volume," *IEEE Trans. Antennas Propag.*, vol. 55, no. 3, pp. 698–706, Mar. 2007.
- [3] J. L. Synge, "Directivity for scalar radiation," *Quarterly Appl. Math.*, vol. 24, no. 1, pp. 90–92, 1966.
- [4] L. Susman and W. K. Kahn, "Measures of beam concentration for scalar radiation," *Radio Sci.*, vol. 5, no. 7, pp. 1091–1097, Jul. 1970.
- [5] E. I. Krupitskii, "On the maximum directivity of antennas consisting of discrete radiators," *Sov. Phys. Dokl.*, vol. 7, pp. 257–259, 1962.
- [6] R. F. Harrington, *Field Computation by Moment Methods*. New York: IEEE Press, 2000, ch. 10.
- [7] D. K. Cheng and F. L. Tseng, "Gain optimization for arbitrary antenna arrays," *IEEE Trans. Antennas Propag.*, vol. 13, pp. 973–974, Nov. 1965.
- [8] S. M. Sanzgeri and J. K. Butler, "Constrained optimization of the performance indices of arbitrary array elements," *IEEE Trans. Antennas Propag.*, vol. 19, no. 4, pp. 493–498, Jul. 1971.
- [9] R. C. Voges and J. K. Butler, "Phase optimization of antenna array gain with constrained amplitude excitation," *IEEE Trans. Antennas Propag.*, vol. 20, no. 4, pp. 432–436, Jul. 1972.
- [10] R. R. Kurth, "Optimization of array performance subject to multiple power pattern constraints," *IEEE Trans. Antennas Propag.*, vol. 22, no. 1, pp. 103–105, Jan. 1974.
- [11] J. Sahalos, "On the optimum directivity of antenna consisting of arbitrarily oriented dipoles," *IEEE Trans. Antennas Propag.*, vol. 24, no. 3, pp. 322–327, May 1976.
- [12] A. I. Uzkov, "An approach to the problem of optimum directive antenna design," *Dokl. Akad. Nauk. SSSR*, vol. 53, pp. 35–38, 1946.
- [13] S. Hwang, A. Medouri, and T. K. Sarkar, "Signal enhancement in a near-field MIMO environment through adaptivity on transit," *IEEE Trans. Antennas Propag.*, vol. 53, no. 2, pp. 685–693, Feb. 2005.
- [14] S. P. Morgan, "Interaction of adaptive antenna arrays in an arbitrary environment," *Bell Syst. Tech. J.*, vol. 44, pp. 23–47, 1965.
- [15] W. F. Young, E. F. Kuester, and C. L. Holloway, "Optimized Arbitrary Wireless Device Arrays for Emergency Response Communications Mar. 2005 [Online]. Available: <http://boulder.nist.gov/div818/81802/MetrologyForWirelessSys/index.html> or http://nvl.nist.gov/nist_pub_search.cfm?type=keyword, NIST Tech. Note 1538, Boulder, CO
- [16] M. I. Skolnik and D. D. King, "Self-phasing array antennas," *IEEE Trans. Antennas Propag.*, vol. 12, no. 2, pp. 142–149, Mar. 1964.
- [17] L. D. DiDomenico and G. M. Rebeiz, "Digital communications using self-phased arrays," *IEEE Trans. Microw. Theory Tech.*, vol. 49, no. 4, pp. 677–684, Apr. 2004.
- [18] W. F. Young, "Optimizing Arrays of Randomly Placed Wireless Transmitters With Receivers Located in the Array Volume," Ph.D. dissertation, Univ. Colorado, Boulder, CO, 2006.
- [19] *Lorch Microwave*, [Online]. Available: <http://www.lorch.com>
- [20] *Diaco*, [Online]. Available: <http://www.daico.com>
- [21] *Advanced Control Components*, [Online]. Available: <http://www.advanced-control.com>



William F. Young (M'06) was born in Ponape, Micronesia, in 1966. He received the B.S. degree in electronic engineering technology from Central Washington University, Ellensburg, WA, in 1992, the M.S. degree in electrical engineering from Washington State University at Pullman, in 1998, and the Ph.D. degree from the University of Colorado at Boulder, in 2006.

Since 1998, he has worked for Sandia National Laboratories in Albuquerque, NM. His work at Sandia focused on the analysis and design of cyber security mechanisms for both wired and wireless communication systems used in the National Infrastructure and the Department of Defense. He has also been a Guest Researcher at the National Institute of Standards and Technology in Boulder, CO, and is working on improving wireless communication systems for emergency responders. His current research interests are in electromagnetic propagation for wireless systems, and the impacts of the wireless channel on overall communication network behavior.



Edward F. Kuester (S'73–M'76–SM'95–F'98) received the B.S. degree from Michigan State University, East Lansing, in 1971, and the M.S. and Ph.D. degrees from the University of Colorado at Boulder, in 1974 and 1976, respectively, all in electrical engineering.

Since 1976, he has been with the Department of Electrical and Computer Engineering at the University of Colorado at Boulder, where he is currently a Professor. In 1979, he was a Summer Faculty Fellow at the Jet Propulsion Laboratory, Pasadena, CA. From 1981 to 1982, he was a Visiting Professor at the Technische Hogeschool, Delft, The Netherlands. In 1992 and 1993, he was an Invited Professor at the École Polytechnique Fédérale de Lausanne, Switzerland. He has held the position of Visiting Scientist at the National Institute of Standards and Technology (NIST), Boulder, CO in 2002, 2004, and 2006. His research interests include the modeling of electromagnetic phenomena of guiding and radiating structures, applied mathematics and applied physics. He is the coauthor of one book, author of chapters in two others, and has translated two books from Russian. He is co-holder of two U.S. patents, and author or coauthor of more than 60 papers in refereed technical journals.

Dr. Kuester is a member of the Society for Industrial and Applied Mathematics (SIAM) and Commissions B and D of the International Union of Radio Science (URSI).



Christopher L. Holloway (S'86–M'92–SM'04) was born in Chattanooga, TN, on March 26, 1962. He received the B.S. degree from the University of Tennessee at Chattanooga, in 1986 and the M.S. and Ph.D. degrees from the University of Colorado at Boulder, in 1988 and 1992, respectively, both in electrical engineering.

During 1992, he was a Research Scientist with Electro Magnetic Applications, Inc., in Lakewood, CO. His responsibilities included theoretical analysis and finite-difference time-domain modeling of various electromagnetic problems. From fall of 1992 to 1994, he was with the National Center for Atmospheric Research (NCAR) in Boulder, CO. While at NCAR his duties included wave propagation modeling, signal processing studies, and radar systems design. From 1994 to 2000, he was with the Institute for Telecommunication Sciences (ITS) at the U.S. Department of Commerce in Boulder, where he was involved in wave propagation studies. Since 2000, he has been with the National Institute of Standards and Technology (NIST), Boulder, where he works on electromagnetic theory. He is also on the Graduate Faculty at the University of Colorado at Boulder. His research interests include electromagnetic field theory, wave propagation, guided wave structures, remote sensing, numerical methods, and EMC/EMI issues.

Dr. Holloway is a member of Commission A of the International Union of Radio Science (URSI). He was awarded the 2006 Department of Commerce Bronze Medal for his work on radio-wave propagation, the 1999 Department of Commerce Silver Medal for his work in electromagnetic theory, and the 1998 Department of Commerce Bronze Medal for his work on printed circuit boards. He is an Associate Editor for the IEEE TRANSACTIONS ON ELECTROMAGNETIC COMPATIBILITY. He was the Chairman for the Technical Committee on Computational Electromagnetics (TC-9) of the IEEE Electromagnetic Compatibility Society from 2000 to 2005. He is currently serving as an IEEE Distinguished lecturer for the EMC Society.